NASA TM X-763

NASA TM X-763

TECHNICAL MEMORANDUM

X-763

STATIC STABILITY AND LONGITUDINAL CONTROL CHARACTERISTICS OF A LENTICULAR-SHAPED REENTRY VEHICLE AT MACH NUMBERS OF 3.5 AND 4.65

By John T. McShera, Jr., and Jerry L. Lowery

Langley Research Center
Langley Station, Hampton, Va.

NATIONAL AERONAUTICS AND SPACE ADMINISTRATION

WASHINGTON

March 1963

NATIONAL AERONAUTICS AND SPACE ADMINISTRATION

TECHNICAL MEMORANDUM X-763

STATIC STABILITY AND LONGITUDINAL CONTROL CHARACTERISTICS OF A LENTICULAR-SHAPED REENTRY VEHICLE AT MACH NUMBERS OF 3.5 AND 4.65*

By John T. McShera, Jr., and Jerry L. Lowery

SUMMARY

An investigation of static stability and longitudinal control characteristics of a lenticular-shaped body with combined horizontal-vertical tail surfaces was conducted in the Langley Unitary Plan wind tunnel at Mach numbers of 3.5 and 4.65. The tests were conducted through an angle-of-attack range from -4° to 56° at angles of sideslip of 0° and ±3° with deflections of the horizontal tail of 0°, -16.4°, 9°, and 26.7°.

The results of this investigation show that the vehicle has a maximum lift-drag ratio on the order of 0.85 and a lift-drag ratio on the order of 0.6 under maximum lift conditions at both test Mach numbers.

The body without tail surfaces is unstable up to the maximum lift (angle of attack approximately 52°) condition at both test Mach numbers. The addition and deflection of the tail surfaces is an effective means of control and provides the vehicle with neutral stability up to an angle of attack near 24°; further increases in angle of attack effect a stable condition. The body with or without combined horizontal- and vertical-tail surfaces is directionally stable and has a positive effective dihedral over the entire angle-of-attack range at both test Mach numbers.

INTRODUCTION

Vehicles under consideration for satellite reentry vehicles range from the ballistic type (lift-drag ratio approximately zero) to the glider type (lift-drag ratio approximately 1.5). The glider type has some maneuverability but presents heating and weight problems. The ballistic type of vehicle has reduced heating and weight problems but lacks the maneuverability exhibited by the glider type of vehicle.

*Title, Unclassified.

The lenticular shape of the present investigation is designed to have lift-drag ratios intermediate to the ballistic and glider reentry vehicles. The reentry course for the intermediate-lift-drag-ratio vehicle consists of initial reentry at high angles of attack to minimize aerodynamic heating and, as the velocity decreases, the angle of attack would be decreased to that at the maximum lift-drag ratio at which time the vehicle could maneuver as a low-lift-drag-ratio glider. Further details of this type of reentry may be found in reference 1. The transition from high-angle reentry to a maximum lift-drag-ratio glide could occur in the supersonic speed range. The present investigation was conducted in the Langley Unitary Plan wind tunnel at Mach numbers of 3.5 and 4.65 to determine the static longitudinal and lateral stability characteristics and the effectiveness of the aerodynamic controls for trimming the longitudinal moments of the lenticular-shaped body.

Additional investigations of the static longitudinal stability and control characteristics of the lenticular and similar models at other supersonic and hypersonic Mach numbers have been conducted and are reported in references 2 to 8.

COEFFICIENTS AND SYMBOLS

Lift, drag, and pitching moment are presented about the stability axes and roll, yaw, and side forces are presented about the body axes. The moment center is located on the body center line at 45 percent of the body length aft of the front of the model.

C_m pitching-moment coefficient, $\frac{\text{Pitching moment}}{q_\infty S l}$

$C_{m_{\delta_h}}$ control effectiveness, $\left(\partial C_m/\partial \delta_h\right)_{\delta_h=0}$, per degree

C_L lift coefficient, $\frac{\text{Lift}}{q_\infty S}$

C_D drag coefficient, $\frac{\text{Drag}}{q_\infty S}$

C_l rolling-moment coefficient, $\frac{\text{Rolling moment}}{q_\infty S l}$

C_n yawing-moment coefficient, $\frac{\text{Yawing moment}}{q_\infty S l}$

C_Y side-force coefficient, $\frac{\text{Side force}}{q_\infty S}$

$\frac{\Delta C_l}{\Delta \beta}$ effective dihedral parameter per degree

$\frac{\Delta C_n}{\Delta \beta}$	directional stability parameter per degree
$\frac{\Delta C_Y}{\Delta \beta}$	side-force parameter per degree
L/D	lift-drag ratio
M_∞	free-stream Mach number
p_t	tunnel stagnation pressure, lb/sq in.
q_∞	free-stream dynamic pressure, lb/sq ft
R	Reynolds number per foot
S	planform area, 0.210 sq ft
l	body length, 6.2 inches
α	angle of attack, deg
β	angle of sideslip, deg
δ_h	deflection of combined horizontal and vertical stabilizing surfaces, deg

APPARATUS

Wind Tunnel

The tests were conducted in the high Mach number test section of the Langley Unitary Plan wind tunnel. The tunnel is a variable-pressure return-flow type of tunnel. The test section is 4 feet square and approximately 7 feet long. The nozzle leading to the test section is of the asymmetric sliding-block type, and Mach numbers may be obtained through a range from 2.3 to 4.65 without tunnel shutdown. Reference 9 gives a detailed description of the tunnel.

Models and Instrumentation

Figure 1 shows the lenticular-shaped model which was constructed of wood with aluminum horizontal-vertical stabilizing surfaces. A photograph of the model is shown in figure 2. The lenticular shape was generated by revolving an ellipse about its minor axis. The ratio of the major axis to the minor axis of the ellipse is 2.82. The stabilizing surfaces were combined horizontal—vertical-tail surfaces with a constant thickness of 0.054 inch and had rounded leading edges. The hinge line of the horizontal surfaces was skewed 45° from the plane of symmetry. (See fig. 1.) The deflection δ_h is the rotary angle generated by

the horizontal surface about its hinge line and is considered positive when the trailing edge of the surfaces is deflected downward. The vertical-tail surfaces were rigidly attached to the horizontal-tail surfaces and the entire tail structure including the vertical fins was deflected for longitudinal control. The chord plane of the horizontal surfaces was located 0.567 inch above the center line of the model.

A sketch of the support system and model installation is presented in figure 3. The model was attached to an internally mounted NASA six-component electrical strain-gage balance. The balance was connected to a remotely controlled sector by means of a straight sting. This sector provided an angle-of-attack range from -4° to 56°.

TESTS

The tests were conducted in the high Mach number test section of the Langley Unitary Plan wind tunnel at Mach numbers of 3.5 and 4.65. The angle-of-attack range was from -4° to 56° at angles of sideslip of 0° and $\pm 3^\circ$. Tests were made on the body alone and the body with combined horizontal-vertical tail surfaces at $\delta_h = 0^\circ$; -16.7°, 9°, and 26.7°. The test conditions of Mach number, stagnation pressure, dynamic pressure, and Reynolds number are as follows:

M_∞	p_t, lb/sq in. abs	q_∞, lb/sq ft	R, ft^{-1}
3.50	33	518	3.04×10^6
3.50	53	860	5.29
4.65	54	350	3.04
4.65	88	550	5.29

The dewpoint temperature for all tests was maintained below -30° F to prevent adverse condensation effects. The stagnation temperature was maintained at 175° F for all Mach numbers.

MEASUREMENTS AND ACCURACIES

The data have been corrected for flow angularity, and the deflection of the balance-sting combination due to load has been applied to all angles of attack. No attempt has been made to correct the data for possibility of sting interference. The angles are estimated to be accurate within $\pm 0.1^\circ$.

The accuracy of the individually measured quantities and coefficients based on previous calibrations and repeatability of the data is estimated to be within the following limits:

C_L	±0.014
C_m	±0.003
C_D	±0.006
C_l	±0.001
$M_\infty = 3.5$	±0.015
$M_\infty = 4.65$	±0.05
C_Y	±0.008
C_n	±0.002
β, deg	±0.1
δ_h', deg	±0.5

PRESENTATION OF RESULTS

The results of this investigation are presented in the following figures:

DISCUSSION

Longitudinal Aerodynamic Characteristics

The maximum values of lift-drag ratio obtained for the body without tail surfaces are about 0.75 at $M_\infty = 3.5$ and about 0.70 at $M_\infty = 4.65$. (See fig. 5.) The addition of the tail surfaces at a deflection of 26.7° increases the maximum L/D to about 0.89 at $M_\infty = 3.5$ and about 0.85 at $M_\infty = 4.65$. Corresponding L/D values at maximum lift conditions are about 0.5 for tail-off condition and 0.6 for the tail-on condition at both test Mach numbers.

The body without tail surfaces is essentially unstable up to the maximum lift condition of the body at both test Mach numbers. (See fig. 5.) The

addition of the tail surfaces ($\delta_h = 0$) makes the vehicle neutrally stable up to an angle of attack near 24°; further increases in angle of attack effect a stable condition for the model.

Deflecting the tail surfaces through a range from -16.4° to 26.7° appears to be an effective means of obtaining longitudinal control of the vehicle at the higher test angles of attack for the center-of-gravity location used for this investigation. It further appears that a small forward shift in center of gravity is desirable to obtain a stable configuration at the lower test angles of attack and this in turn would greatly enhance the control effectiveness of the tail surfaces. The control effectiveness is better illustrated in figure 6 which shows the variation of $C_{m_{\delta_h}}$ with angle of attack. There is a small positive degree of control effectiveness at angles of attack to near 25° and beyond this angle of attack there is a significant increase in control effectiveness. Sample curves of the type used to obtain figure 6 are presented as figure 7.

The effects of Reynolds number were investigated between 3.04×10^6 and 5.29×10^6 and, as shown in figure 8, it appears there is little or no effect on the drag or longitudinal characteristics of the configuration.

Lateral Stability Characteristics

The lateral stability parameters were obtained from test data taken over the angle-of-attack range at angles of sideslip of 0° and ±3°. The body without tail surfaces is directionally stable and generally has a positive effective dihedral in the angle-of-attack range of these tests as shown in figure 9. The addition of the tail surfaces ($\delta_h = 0°$) for the most part slightly increases the directional stability and positive effective dihedral over the test angle-of-attack range.

CONCLUSIONS

The investigation of the static stability and longitudinal control characteristics of a lenticular-shaped reentry vehicle at Mach numbers of 3.5 and 4.65 has led to the following conclusions:

1. The vehicle has a maximum lift-drag ratio of the order of 0.85 and a lift-drag ratio on the order of 0.6 at maximum lift conditions at both test Mach numbers.

2. The vehicle is longitudinally neutrally stable (center of gravity at 45 percent body length) at lift coefficients up to those corresponding to the maximum lift-drag ratio; above the maximum lift-drag ratio, however, a marked increase in stability occurs.

3. There is a small degree of longitudinal control at angles of attack up to the maximum lift-drag ratio; however, this control is significantly increased at the higher test angles of attack.

4. For the tests the body with and without tail surfaces is laterally and directionally stable throughout the entire angle-of-attack range at both Mach numbers.

Langley Research Center,
National Aeronautics and Space Administration,
Langley Station, Hampton, Va., November 23, 1962.

REFERENCES

1. Staff of Langley Flight Research Division (Compiled by Donald C. Cheatham): A Concept of a Manned Satellite Reentry Which is Completed With a Glide Landing. NASA TM X-226, 1959.

2. Jackson, Charlie M., Jr., and Harris, Roy V., Jr.: Static Longitudinal Stability and Control Characteristics at a Mach Number of 1.99 of a Lenticular-Shaped Reentry Vehicle. NASA TN D-514, 1960.

3. Letko, William: Experimental Investigation at a Mach Number of 3.11 of the Lift, Drag, and Pitching-Moment Characteristics of Five Blunt Lifting Bodies. NASA TN D-226, 1960.

4. Demele, Fred A., and Lazzeroni, Frank A.: Effects of Control Surfaces on the Aerodynamic Characteristics of a Disk Re-Entry Shape at Large Angles of Attack and a Mach Number of 3.5. NASA TM X-576, 1961.

5. Jaquet, Byron M.: Static Longitudinal and Lateral Stability Characteristics at a Mach Number of 3.11 of Square and Circular Plan-Form Reentry Vehicles, With Some Effects of Controls and Leading-Edge Extensions. NASA TM X-272, 1960.

6. Olstad, Walter B., and Wornom, Dewey E.: Static Longitudinal Stability and Control Characteristics at Mach Numbers of 2.86 and 6.02 and Angles of Attack up to 95° of a Lenticular-Shaped Reentry Vehicle. NASA TM X-621, 1961.

7. Lazzeroni, Frank A.: Aerodynamic Characteristics of Two Disk Re-Entry Configurations at a Mach Number of 2.2. NASA TM X-567, 1961.

8. Rainey, Robert W., Compiler: Summary of Aerodynamic Characteristics of Low-Lift-Drag-Ratio Reentry Vehicles From Subsonic to Hypersonic Speeds. NASA TM X-588, 1961.

9. Anon.: Manual for Users of the Unitary Plan Wind Tunnel Facilities of the National Advisory Committee for Aeronautics, NACA 1956.

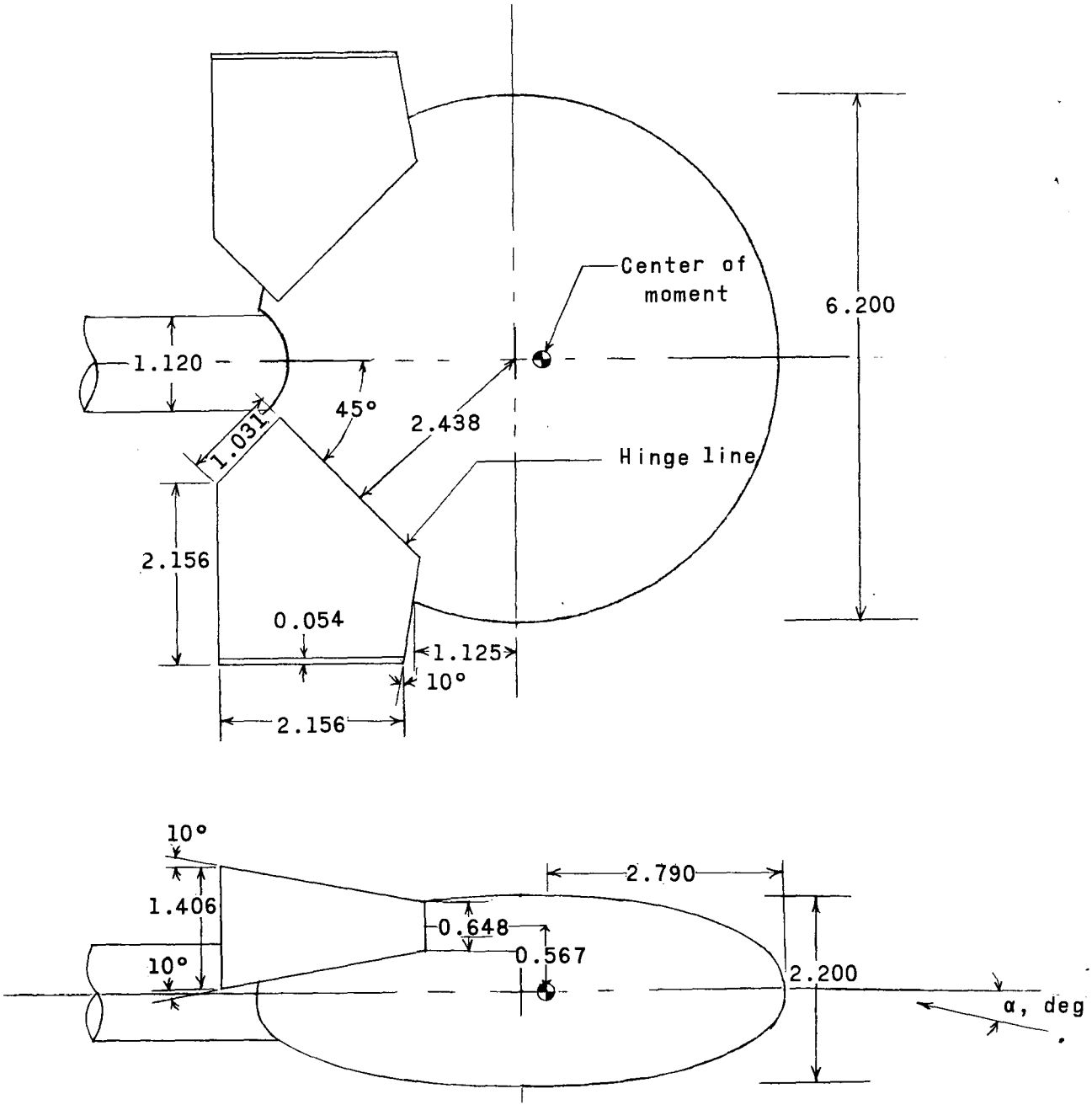

Figure 1.- Drawing of model with horizontal-vertical stabilizing surfaces. Horizontal-tail surface area, 10.22 square inches; vertical-tail surface area, 4.45 square inches. All dimensions are in inches.

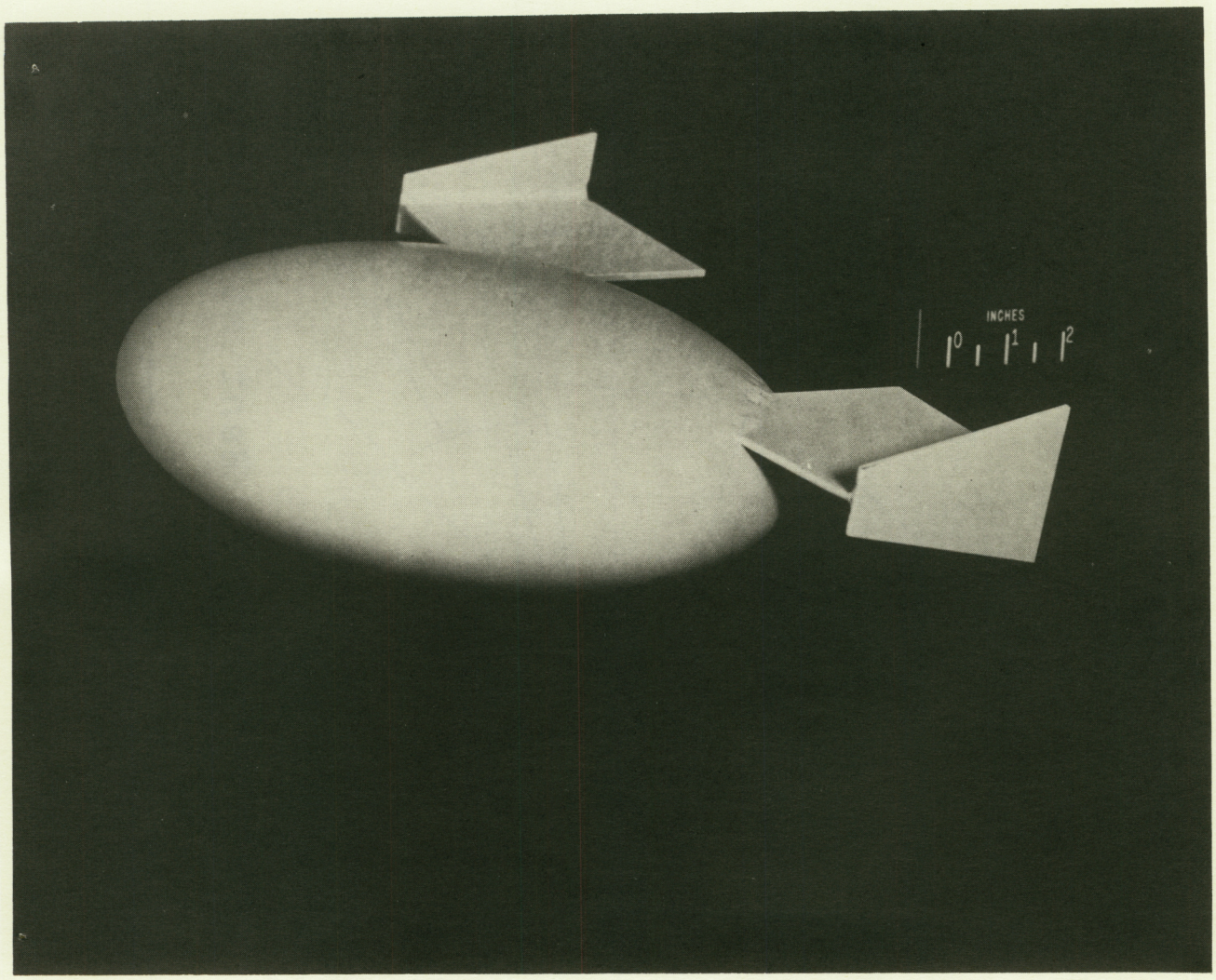

L-60-753

Figure 2.- Photograph of the model with horizontal-vertical stabilizing surfaces.

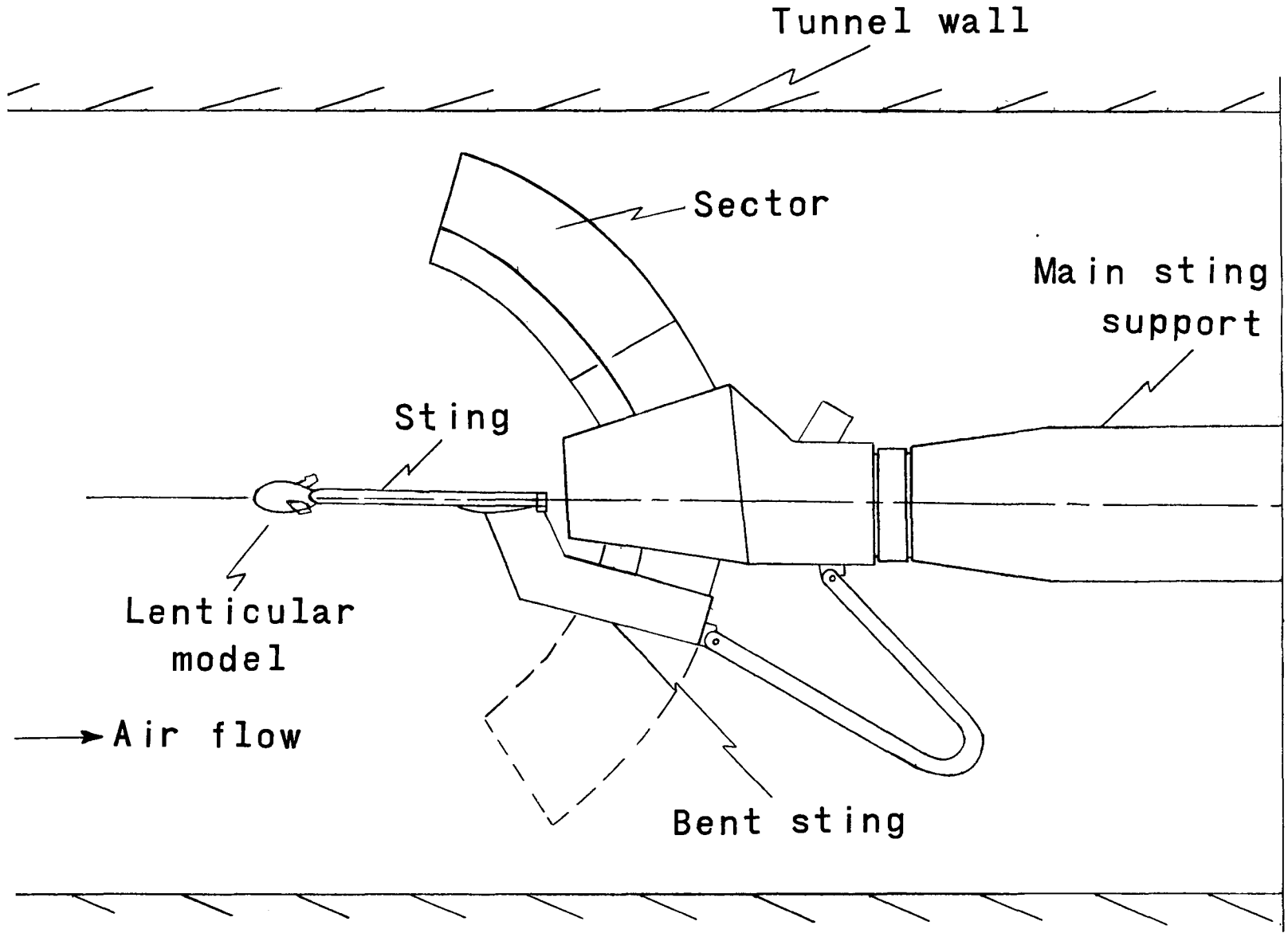

Figure 3.- Sketch of the model support system used during test.

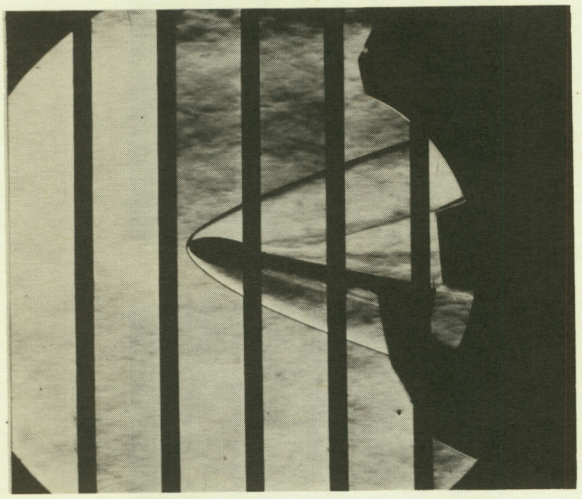

α = 12°

α = 24°

α = 36°

M_∞ = 4.65

α = 48°

(a) Body alone. L-62-7048

Figure 4.- Typical schlieren photographs.

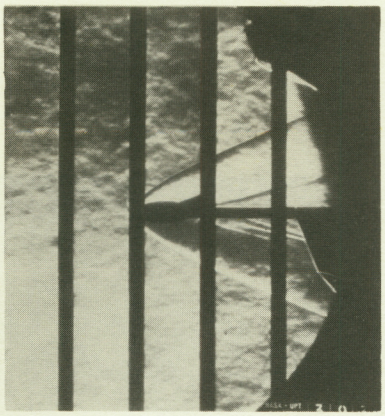

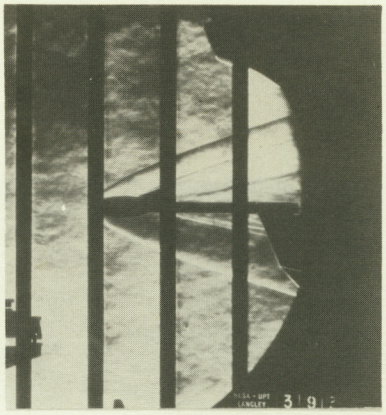

α=0°

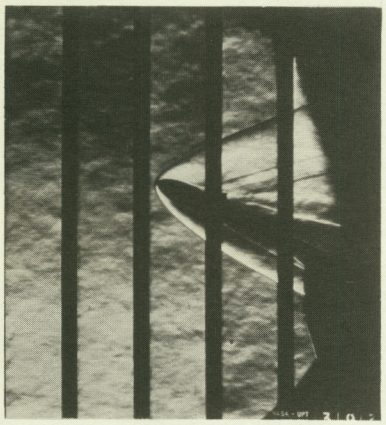

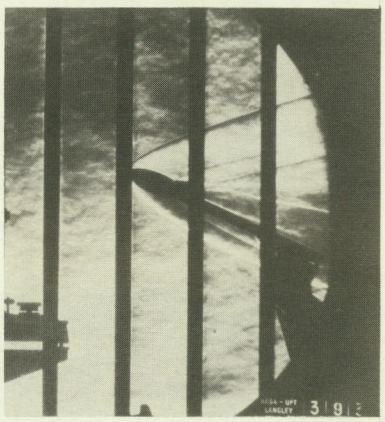

α=24°

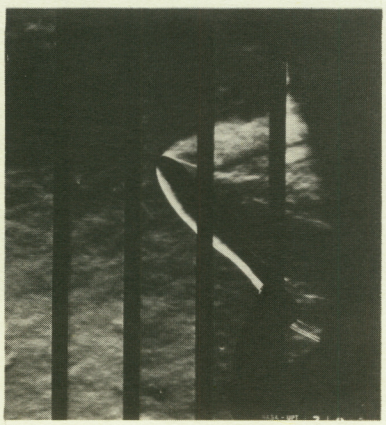

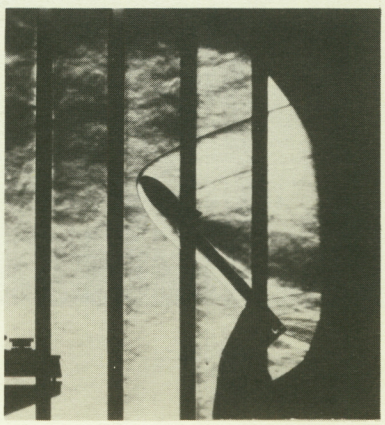

α=48°

$M_\infty=3.50; \delta_h=0°$

$M_\infty=4.65; \delta_h=-16.4°$

(b) Body with horizontal-vertical stabilizing surfaces. L-62-7049

Figure 4.- Concluded.

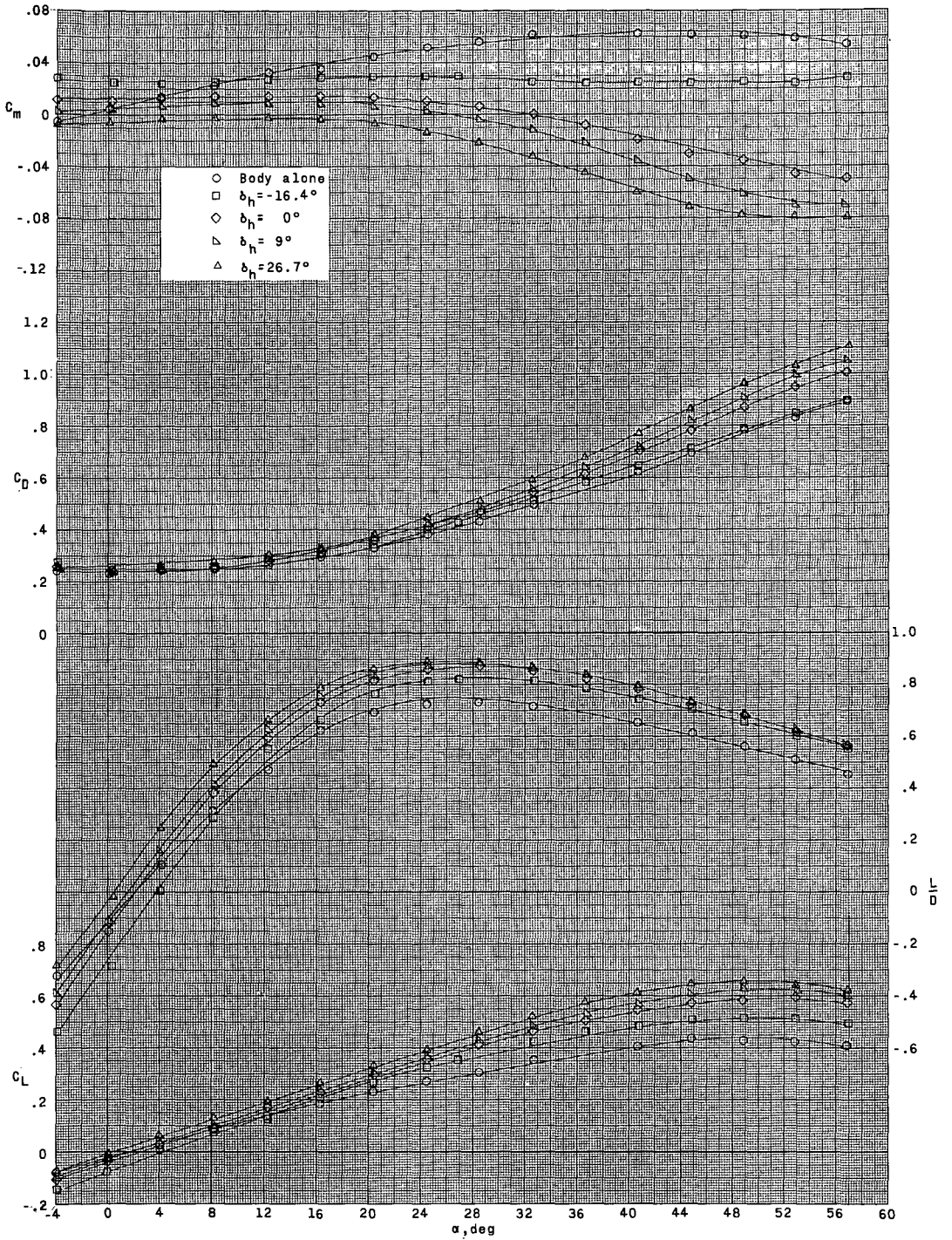

(a) $M_\infty = 3.50$; $R = 3.04 \times 10^6$.

Figure 5.- Longitudinal aerodynamic characteristics of the model at various deflections of the horizontal-vertical stabilizing surfaces.

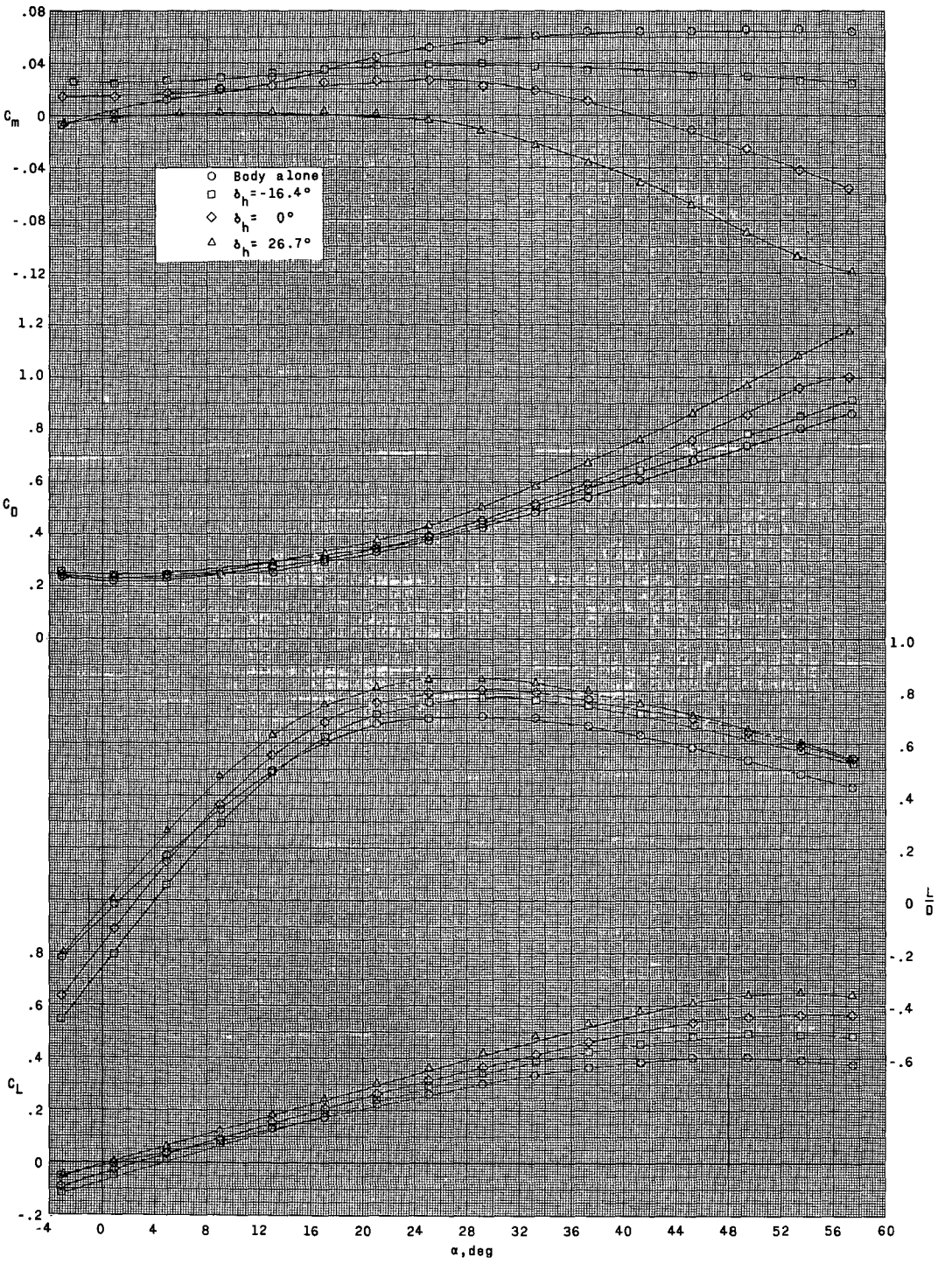

(b) $M_\infty = 4.65$; $R = 3.04 \times 10^6$.

Figure 5.- Concluded.

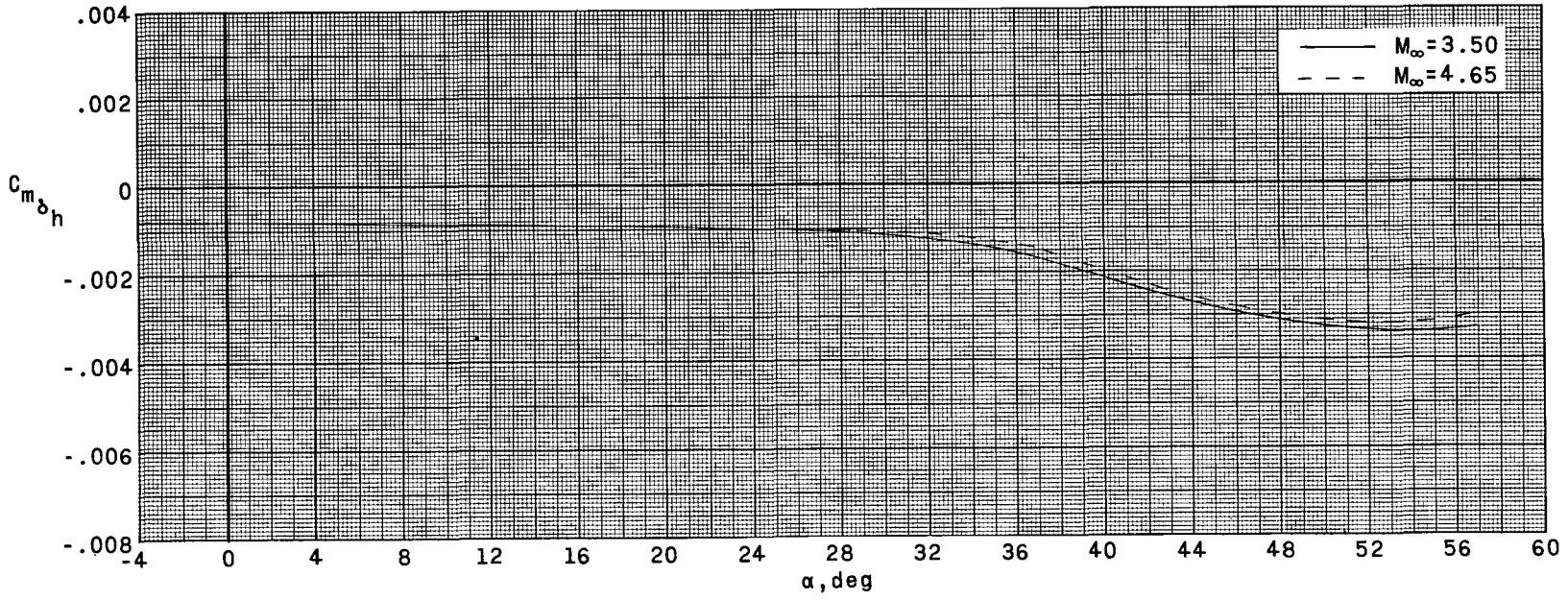

Figure 6.- Control effectiveness at various angles of attack. (Variation of C_m with δ_h taken at $\delta_h = 0^o$.)

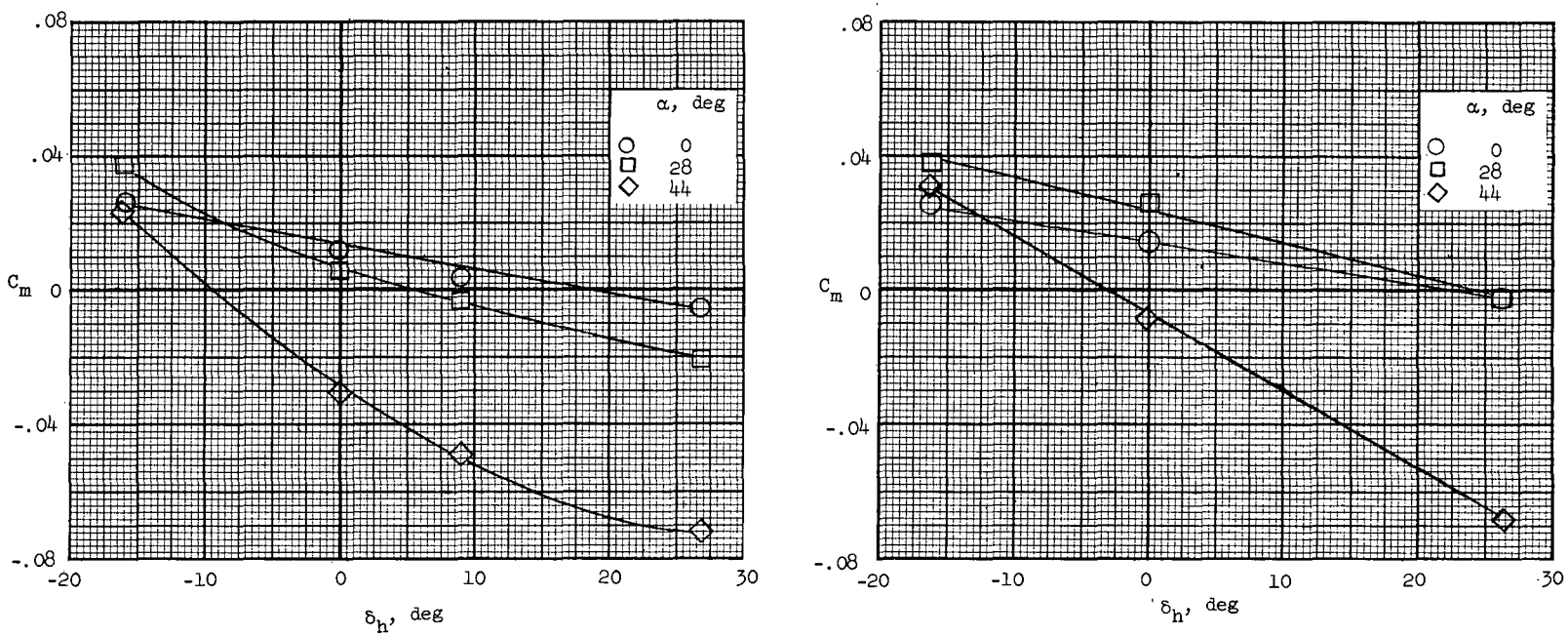

(a) $M_\infty = 3.50$.

(b) $M_\infty = 4.65$.

Figure 7.- Variation of pitching moment with deflections of horizontal-vertical stabilizing surfaces.

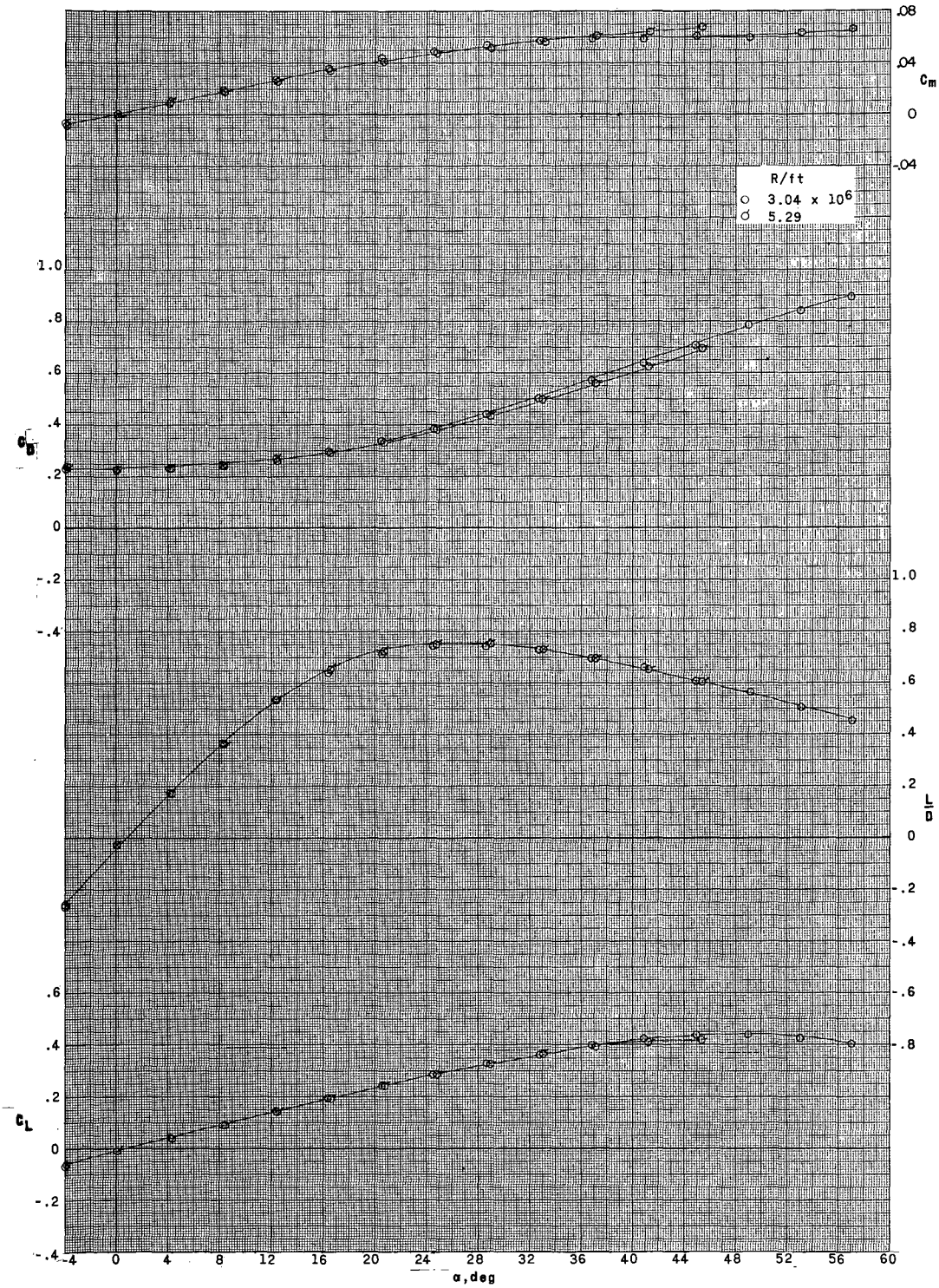

(a) $M_\infty = 3.50$.

Figure 8.- Effect of Reynolds number on the longitudinal aerodynamic characteristics of the body-alone configuration.

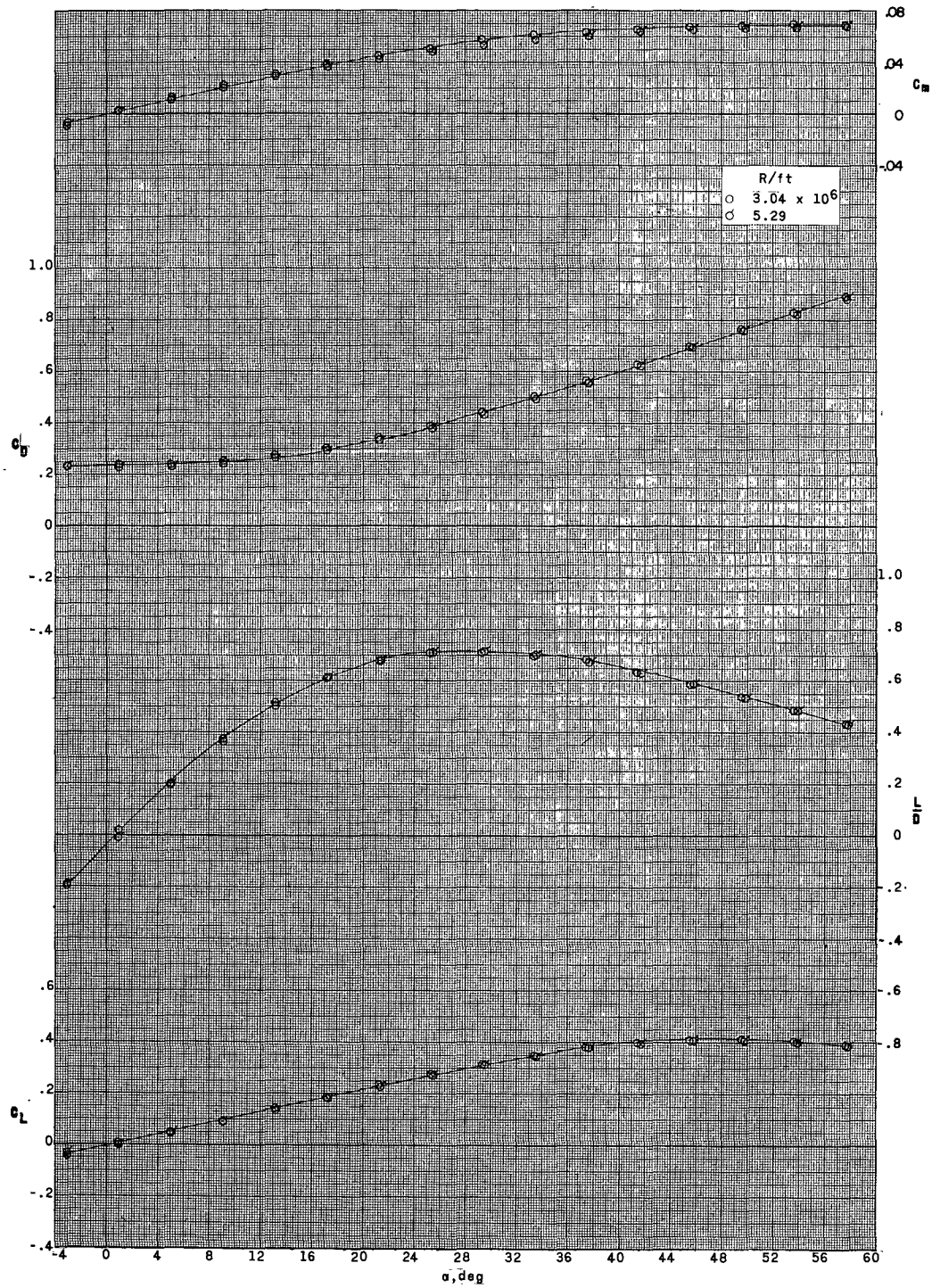

(b) $M_\infty = 4.65$.

Figure 8.- Concluded.

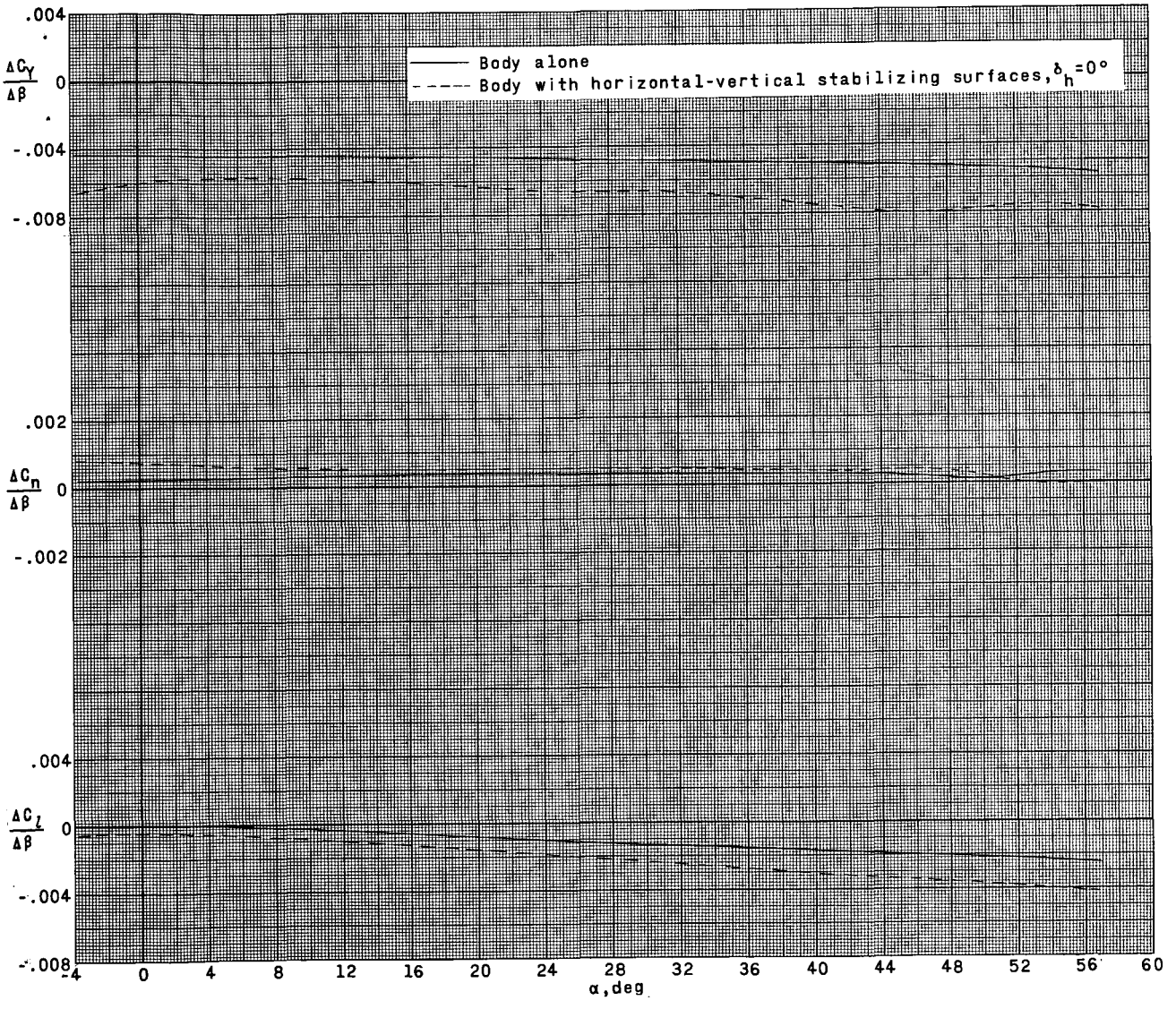

(a) $M_\infty = 3.50$.

Figure 9.- Summary of lateral stability characteristics of the model at various deflections of the horizontal-vertical stabilizing surfaces.

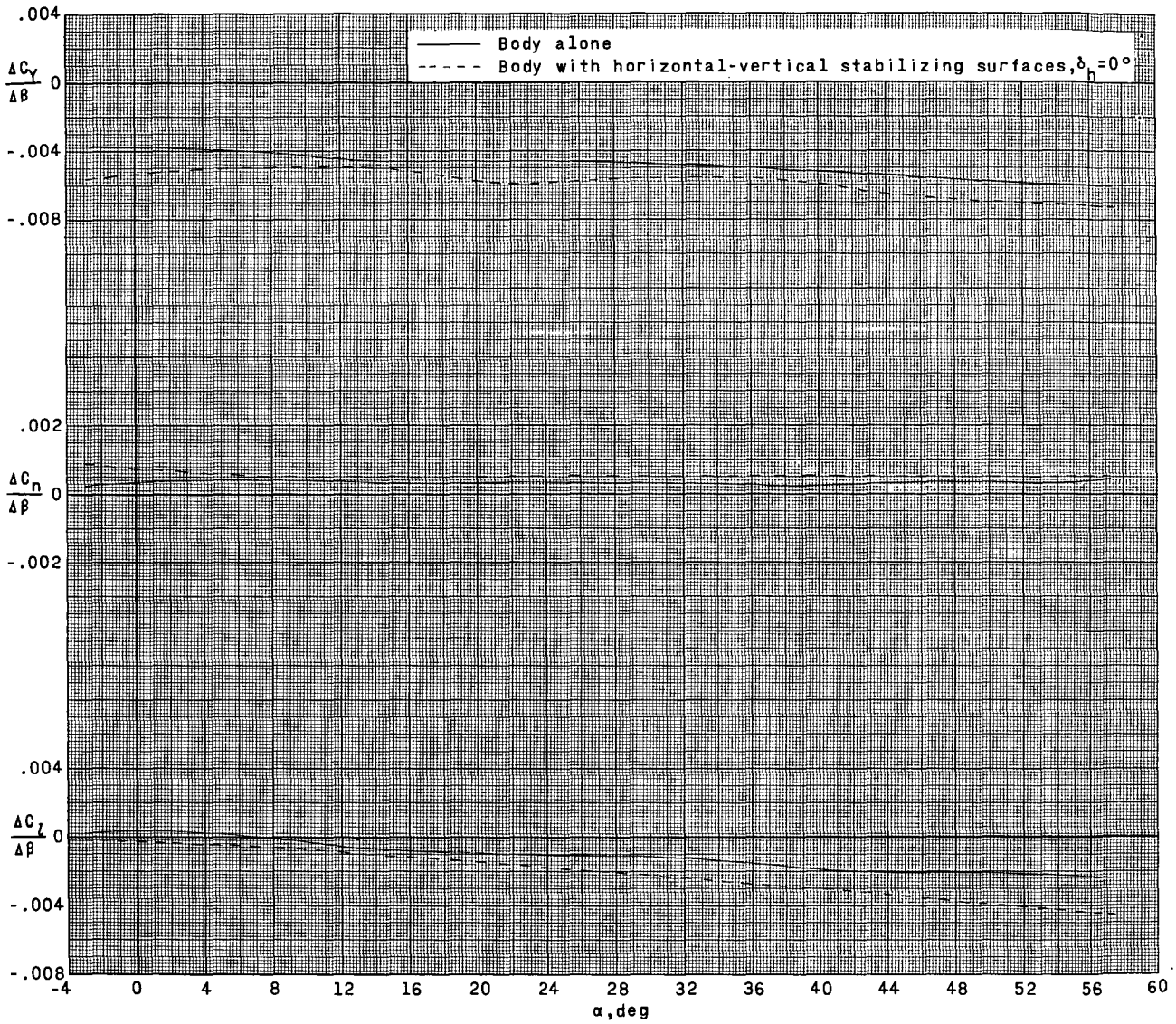

(b) $M_\infty = 4.65$.

Figure 9.- Concluded.